The Effects of Atmospheric Variations on the High Energy Radiation Environment at the Surface of Mars

A. Keating, *Laboratório de Instrumentação e Física Experimental de Partículas, Lisbon, Portugal (keating@lip.pt) and European Space Agency, Noordwijk, The Netherlands*, **M. Pimenta**, *Laboratório de Instrumentação e Física Experimental de Partículas, Lisbon, Portugal,* **A. Mohammadzadeh, P. Nieminen, J. -P. Huot**, **E. Daly**, *European Space Agency, Noordwijk, The Netherlands.*

Introduction:

A modelling framework for the prediction of the Martian high-energy radiation environment and its interface with the European Mars Climate Database (EMCD) was developed [1]. Models features include input solar cycle modulated cosmic ray and solar particle event spectra, both based on CREME-96, the transport of this radiation in the Martian atmosphere and regiolith, including creation of secondary radiation, using the Geant4 Monte-Carlo toolkit[2]. Details of the atmosphere are derived from the European Mars Climate Database with a dense topological grid and layering of the atmosphere. Seasonal and diurnal variations are considered for different location. Surface topology is derived from the Mars Orbiter laser altimeter (MOLA) and geology is modelled. The outputs are full energetic particle transport histories, maps of radiation fluxes and doses.

The Martian climatological fields (atmospheric temperature, water column density) vary strongly with season, local time, and location. In this paper we investigate how the radiation environment at the surface of Mars varies with seasonal atmospheric changes. Dust scenarios were considered, by evaluation of atmospheric density changes.

European Mars Climate Database:

The EMCD contains data on temperature, wind, density, pressure, radiative heat fluxes, and other parameters, resulting from global circulation model simulations, stored on a 5°x5°, longitude-latitude grid from the surface up to an altitude of approximately 120 km (above 120 km, pressure and density can be estimated using the database access software) [3]. Altitudes are defined with respect to local topological elevations.

The vertical coordinate for the 3D spatial variables is defined as $\sigma = p/p_0$, where p is the atmospheric pressure and p_0 is the local surface pressure, also stored in the database. Thus, σ is 1 at the surface and 0 at infinity and the σ levels follow the model topography. There are 32 σ levels from 5m up to around 120 km [3] delineating atmospheric layers.

Wind, temperature, pressure and other fields are averaged and stored for 12 Martian Universal Times at longitude 0°, for 12 Martian "seasons" to give a comprehensive representation of the annual and diurnal cycles. [3][4]

An interface has been built in order to read EMCD data as input for the Geant4 simulation Geometry Construction class, for each location, time and solar longitude.

Figure 1 shows the EMCD Viking dust scenario daily-averaged pressure from the Viking sites. An estimate of the variability due to weather systems, with the seasonal trend component of the EMCD variance removed, is also shown. The seasonal cycle is due largely to the condensation and sublimation of CO_2, although there is an important dynamical component [4], while the high-frequency oscillations are due to weather systems passing over the Landers [4].
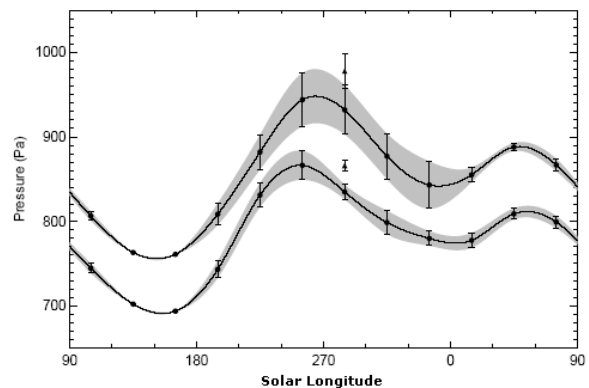
Figure 1 - Pressure at the Viking 1[1] (bottom curve) and 2[2] (top curve) sites for 1 year of the EMCD Viking dust scenario [4]

Topology and Geology

The mapping of the radiation environment of a planet based on σ layer calculations is highly dependent on its topology. For that reason the interface extracts the Martian surface altitude from the MOLA instrument on board NASA's Mars Global Surveyor (MGS) spacecraft [5].

Mars' geology also plays a very important role in the radiation environment characterization. The Martian atmosphere, being of very low density (maximum values of the order of 10^{-2} kgm^{-3}), behaves as a "soft" medium for incoming energetic radiation, which is therefore able to reach the Martian surface. As a result there is an important contribution from secondary radiation particles generated and backscattered at the surface.

The average density of Mars' soil is about 3.75 g

---

[1] Viking lander 1 was situated at 22ºN, 48ºW.

[2] Viking lander 2 was situated at 48ºN, 226ºW.

cm^{-3} and the mantle and crust bulk composition consist mainly of silicon dioxide and iron oxides [6]. Sub-surface water and ice, for which recent evidence has been produced, are expected to have an effect on backscatter properties, and they can easily be introduced later into the framework.

Input radiation

In interplanetary space the radiation sources are solar X-rays, Solar Energetic Particles (SEP), consisting of protons and other ions, energetic electrons originating in Jupiter's magnetosphere, Galactic Cosmic Rays (GCR) and galactic X-rays and gamma-rays. However, for Mars-orbiting and landing missions the radiation environment is mainly due to GCRs and SEPs [1].

GCR input fluxes were considered for the "maximum" phase of the solar cycle, but with "quiet" interplanetary conditions. The inputs were derived from the CREME96 model [7]. This model represents the environment that prevails in the absence of solar energetic particle events for near-Earth interplanetary locations [7], [8]. These interplanetary flux models are based on measurements at Earth (1AU*) [7]. Its intensity varies over a 22-years solar cycle [8]. The phasing with respect to the solar cycle corresponds to the foreseen European Mars mission ExoMars [9] expected launched in 2011.

Radiation Transport Simulation Set-up

The geometry implemented in the Geant4 simulation takes into account: a) The geographical grid size given by the 5°x5° resolution of EMCD, b) The average composition of the soil of 30% Fe_2O_3 and 70% SiO_2, with density 3.75 g cm^{-3}, c) The thickness of the soil is calculated according to the proton total penetration depth and the MOLA surface elevation, d) The thickness of the 32 atmospheric layers given by the σ levels of EMCD, e) A fixed atmospheric composition consisting of: CO_2, N_2, Ar, O_2, CO and H_2O [6] f) The density, temperature and pressure of the 32 atmospheric layers computed from EMCD. However, these parameters are all easily adapted to account for future improvement in knowledge (e.g. sub-surface water/ice).

Different geometries, different location and times of the day

Each location (Longitude, Latitude) on the Martian surface, each phase of the Martian year (solar longitude) or each time of the Martian day corresponds to a specific set of atmospheric properties. For this reason each of them corresponds to specific simulation geometry. All simulation cases (Cases A to I) referred to in the subsequent sections are defined in Table I.

---

* Medium Earth-Sun distance corresponds to approximately 150x10^6 km.

The simulated cases presented in this paper are located: a) in the cliff of Olympus Mons (MO) volcano; and b) Tyrrhena Paterae (TP), one of the three large, ancient, low relief broad mountain of volcanic origin that have developed along faults that surrounds Hellas Basins [6].

TABLE I
SIMULATED CASES

Case	Long (E)	Lat (N)	Name	Solar Longitude	Time[1] (Hours)
A	75	-7.5	(TP)	180°-210°	12
B	80	-7.5	(TP)	180°-210°	02
C	80	-7.5	(TP)	180°-210°	12
D	80	-7.5	(TP)	180°-210°	22
E	80	-12.5	(TP)	180°-210°	12
F	-105	22.5	(OM)	180°-210°	12
G	-140	22.5	(OM)	180°-210°	02
H	-140	22.5	(OM)	180°-210°	12
I	-140	22.5	(OM)	180°-210°	22

[1] At Longitude 0°

Simulation Results

The Monte-Carlo transport of 10^5 protons through the Martian atmosphere and surface has been incorporated into the simulation. Particles are generated at the top of a column of the atmosphere of 5° x 5°. All primary and secondary particles are tracked from the generation point until they are absorbed, "killed" or reach geometry tracking limits (generally meaning having lost most of their energy). The fluences of all different particles were analysed as well as the dependence on the local atmospheric properties such as density, pressure and temperature. A strong dependence of the fluences on surface pressure was verified as illustrated on the following subsections that summarise the results obtained.

Primary and secondary particles

Figure 2 illustrates how the fluence of protons at the surface of Mars varies with the surface pressure. It can be seen that the primary proton fluence at the surface decreases with the atmospheric pressure at the surface. On the other hand the fluence of secondary protons is expected to increase with increasing surface pressure. This result is attributed to the denser air column that primary particles travel through for higher mean surface pressure. Consequently the probability of interaction, absorption and spallation in the atmosphere increases with increasing surface pressure. For the same reason the fluence of secondary particles is expected to increase with increasing surface pressure. This can also be verified in the in figure 3.
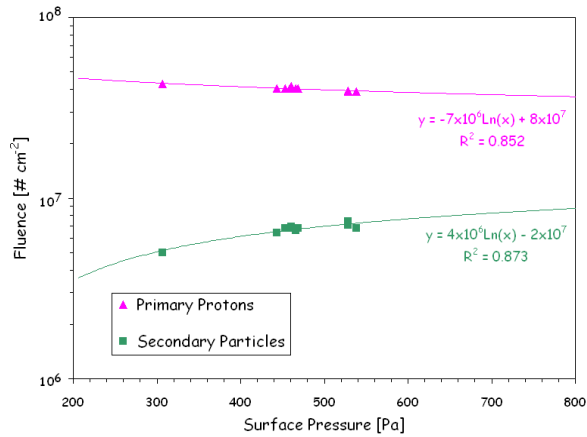
Figure 2 –Transfer function for integrated fluence of protons at the surface of Mars.

Figure 3 shows the dependence of the fluence at the surface of Mars of secondary electrons; direct incident secondary neutrons; ions and photons with the surface pressure.
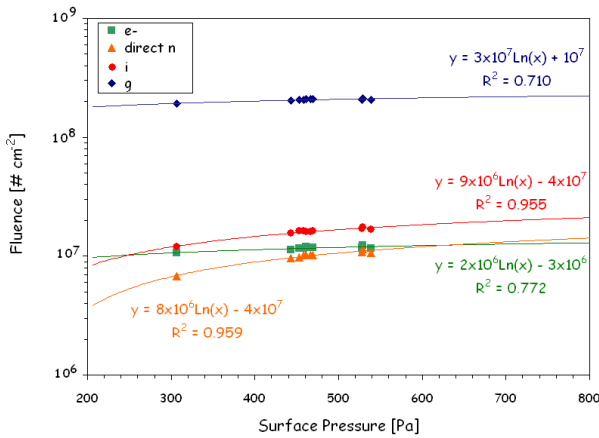
Figure 3–Transfer function for integrated fluence of secondary particles at the surface of Mars.

Backscattered Neutrons

Figure 4 illustrates the important contribution from backscattered neutrons at the surface and shows the inverse relationship between surface pressure and the relative importance of backscattered neutrons detected at the surface of Mars.
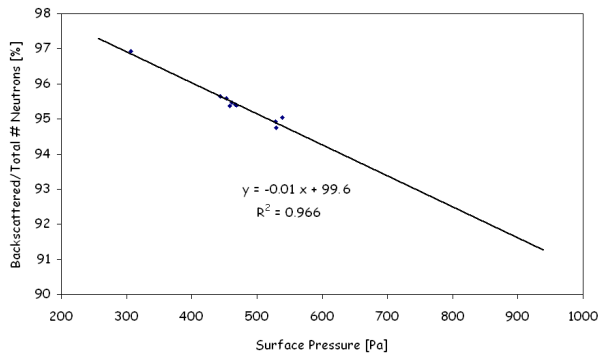
Figure 4 –Impact of surface pressure in the percentage of Backscattered neutrons.

Pressure as function of Solar Longitude

Figure 5 compares the surface pressure at the Viking 1 (thick solid curve) and 2 (top curve) sites for 1 year of the EMCD Viking dust scenario obtained from [3], and the average of the overall surface pressure calculated from EMCD for different solar longitudes (dashed curve).
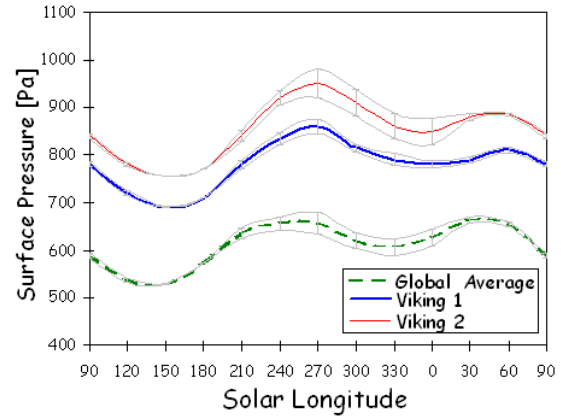
Figure 5 – Surface pressure as function of Solar Longitude for different locations.

Integrated fluence as function of Solar Longitude

Figure 6 illustrates the total integrated fluence of all detected particles at the surface of Mars expected at Viking1 and 2 sites and the estimated average integrated fluence of all detected particles at the surface of Mars.
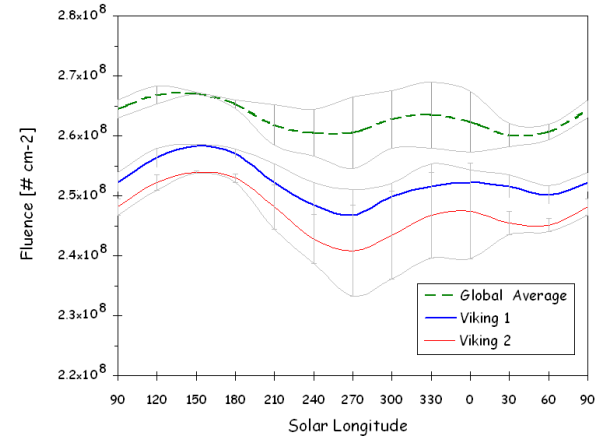
Figure 6–Total integrated fluence as function of Solar Longitude for different locations.

Conclusions

Results presented here show that the framework developed is capable of predicting the high-energy radiation environment at the surface of Mars for different locations and solar longitudes. The model also shows the relative importance of the backscattered neutron component of the radiation environment. A first trial for a transfer function for radiation environment prediction is presented.

The dust density is typically less than 10^{-3} g/cm^2 which means less than 0.5×10^{-3}% of the atmospheric density. For this reason the impact of different dust scenarios is not expected to be very significant.

The framework will be very valuable for planning future mars missions and estimating the effects on lander systems, as well as predicted expected instrument behaviour.

References

[1] A.Keating, et al, "A Model for Mars Radiation Environment Characterization", *NSREC*, Seattle, USA, 12th July, 2005 (accepted to IEEE-TNS).

[2] S Agostinelli et al, "Geant4-A simulation toolkit", *Nucl Instrum Meth Phys Res.*, A506, Issue 3, 2003, pp. 250-303.

[3] F.Forget. (2001, May 18). *What is the Mars Climate Database?* Avilable: http://www-mars.lmd.jussieu.fr/

[4] S.R.Lewis, M.Collins, and P.L.Read, "A climate database for Mars", *Journal of Geophysical Research–Plane*ts, vol. 104, no. E10, pages 24,177–24,194 (1999).

[5] James B. Abshire, Xiaoli Sun, Robert S. Afzal. (1999, August). Mars Orbiter Laser Altimeter Receiver Model and Performance Analysis. *NASA Goddard Space Flight Center Laser Remote Sensing Branch*. Available: http://pds-geosciences.wustl.edu/geodata/mgs-m-mola-3-pedr-l1a-1/mgsl_21xx/document/calib.pdf

[6] Joseph M. Boyce, *The Smithsonian Book of Mars*, Smithsonian Institution Press, 2002, 88-125.

[7] A.J.Tylka (2003, December 15). *Orbit Selection on CREME96 for Flux*. Available: https://creme96.nrl.navy.mil/cm/FluxOrbit.htm

[8] A.J.Tylka et al, "CREME96: A revision of the Cosmic Ray Effects on Micro-Electronics Code", *IEEE Transitions on Nuclear Science*, 1997, vol. 44, pp.2150-2160.

[9] ESA. (2005, August 4). *Aurora Exploration Program*. Available: http://www.esa.int/SPECIALS/Aurora/SEM1NVZKQAD_0.html.